Self-awareness control effect of cooperative epidemics on complex networks

Cite as: Chaos **29**, 053123 (2019); https://doi.org/10.1063/1.5063960
Submitted: 03 October 2018 . Accepted: 23 April 2019 . Published Online: 21 May 2019

Zexun Wang, Ming Tang, Shimin Cai, Ying Liu, Jie Zhou, and Dingding Han

Self-awareness control effect of cooperative epidemics on complex networks

Cite as: Chaos **29**, 053123 (2019); doi: 10.1063/1.5063960
Submitted: 3 October 2018 · Accepted: 23 April 2019 ·
Published Online: 21 May 2019

Zexun Wang,[1,2,3] Ming Tang,[1,3,4,a)] Shimin Cai,[2,3,b)] Ying Liu,[3,5] Jie Zhou,[6] and Dingding Han[7]

AFFILIATIONS

[1]School of Information Science Technology, East China Normal University, Shanghai 200241, China
[2]Web Sciences Center, University of Electronic Science and Technology of China, Chengdu 611731, China
[3]Big Data Research Center, University of Electronic Science and Technology of China, Chengdu 611731, China
[4]Shanghai Key Laboratory of Multidimensional Information Processing, East China Normal University, Shanghai 200241, China
[5]School of Computer Science, Southwest Petroleum University, Chengdu 610500, China
[6]School of Physics and Materials Science, East China Normal University, Shanghai 200241, China
[7]School of Information Science and Technology, Fudan University, Shanghai 200433, China

[a)]tangminghan007@gmail.com
[b)]shimin.cai81@gmail.com

ABSTRACT

Coinfection mechanism is a common interacting mode between multiple diseases in real spreading processes, where the diseases mutually increase their susceptibility, and has aroused widespread studies in network science. We use the bond percolation theory to characterize the coinfection model under two self-awareness control strategies, including immunization strategy and quarantine strategy, and to study the impacts of the synergy effect and control strategies on cooperative epidemics. We find that strengthening the synergy effect can reduce the epidemic threshold and enhance the outbreak size of coinfected networks. On Erdős–Rényi networks, the synergy effect will induce a crossover phenomenon of phase transition, i.e., make the type of phase transition from being continuous to discontinuous. Self-awareness control strategies play a non-negligible role in suppressing cooperative epidemics. In particular, increasing immunization or the quarantine rate can enhance the epidemic threshold and reduce the outbreak size of cooperative epidemics, and lead to a crossover phenomenon of transition from being discontinuous to continuous. The impact of quarantine strategy on cooperative epidemics is more significant than the immunization strategy, which is verified on scale-free networks.

Multiple epidemics spreading interactively is a common phenomenon in the real world and has attracted more and more attention. A common interacting mode between two pathogens is called coinfection, where the pathogens mutually increase their susceptibility, e.g., the coinfection of the Spanish flu and pneumonia in 1918 and the coinfection of the tuberculosis pathogen and human immunodeficiency virus. The coinfection may induce a discontinuous phase transition of epidemic spreading on some networks, where the number of infected nodes jumps from zero to a large value suddenly. This sudden jump cannot give us any sign of warning such as fluctuations, which will bring more panic and injury to the human society. How to suppress effectively the discontinuous phase transition and the spread of diseases is an important issue in the cooperative epidemics. Considering that a node infected by the first disease has a high risk of infection by the second disease, we propose a self-awareness control strategy in the cooperative epidemics. In this strategy, a node infected with one disease will be immunized or quarantined based on self-awareness of infection risk. We develop a percolation-based framework to theoretically analyze how these control strategies affect the cooperative spreading epidemics. In terms of controlling diseases, both strategies can remarkably suppress the cooperative epidemics and transform the type of phase transition from being discontinuous to continuous. Compared with the immunization strategy, the suppressing effects of quarantine strategy on cooperative epidemics are more significant. The cooperative spread of disease can be mapped to news and rumors, thus the results of this paper provide a theoretical guarantee for how to control the pervasion of epidemics and rumors.

I. INTRODUCTION

Throughout human history, infectious diseases have always been threatening human health. Once a disease becomes epidemic, it will cause enormous economic loss. For the prediction and prevention of epidemic spreading, scientists from different disciplines are studying on the mathematical modeling of infectious diseases.[1,2] As real disease spreading is not always in isolation, multiple epidemics spreading interactively have attracted more and more attention.[3–8] A common interacting mode between two pathogens is called coinfection, where the pathogens mutually increase their susceptibility.[9,10] As early as 1918, cooperative epidemics was discovered from the coinfection of the Spanish flu and pneumonia.[11] Such phenomenon was further found in the coinfection of the tuberculosis (TB) pathogen and human immunodeficiency virus (HIV).[12–14] In particular, the HIV promotes the possibility of TB from incubation to activation, and an active TB case has a much higher incidence of HIV.

Cooperative epidemics is one of the research hotspots in spreading dynamics on complex networks in recent years.[9,10,15–23] Newman and Ferrario presumed an asymmetric cooperation rule between two diseases,[9] where the propagation of the first disease is independent of the second, but the second disease can only spread among the nodes infected by the first disease.[15] Then, a symmetric coinfection rule was proposed to describe real cooperative mechanism in multiple epidemics.[10,16–20] Chen *et al.* studied the cooperative coinfection of SIR (susceptible–infected–removed) spreading of two diseases and found that a strong cooperation of coinfection mechanism may induce a discontinuous phase transition.[10,16,17] Whether the coinfection of multiple diseases is a discontinuous phase transition depends on the underlying network structure. This is a major reason why a continuous phase transition occurs on two-dimensional lattices and scale-free networks, while a discontinuous phase transition occurs on four-dimensional lattices and homogeneous networks.[16,17] In Refs. 18 and 19, the SIS model under the symmetric rule was studied. Hébert-Dufresne *et al.* related the coinfection model with the aggregation of networks and found that the aggregation of networks, as a means of suppressing the spread of a single disease, can promote the spread of disease and results in a discontinuous phase transition.[18] Chen *et al.* revealed that the coinfection induces a hysteresis phenomenon for the SIS cooperative epidemics spreading on stochastic networks.[19] This coinfection mechanism was also introduced into multiplex overlapped networks, and the interlayer synergistic effect leads to a crossover phenomenon of phase transition from being continuous to being discontinuous.[20]

As mentioned above, coinfection may induce a discontinuous phase transition of epidemic spreading on some networks, where the number of infected nodes jumps from zero to a large value suddenly. This sudden jump cannot give us any sign of warning such as fluctuations, which will bring more panic and injury to the human society. Therefore, how to suppress effectively the discontinuous phase transition is an important issue in the cooperative epidemics.[24,25] In the dynamics of epidemic, it is very significant to control the spread of disease, and many different strategies have been proposed.[26–28] To this end, we need to know the underlying contact network structure and its infection status in time and identify which nodes should be controlled.[29] However, it is very difficult to timely obtain these information in real epidemic spreading processes.[30,31] Considering that a node infected by the first disease has a high risk of infection by the second disease, we propose a self-awareness control strategy in the cooperative epidemics. In this strategy, a node infected with one disease will be immunized or quarantined based on self-awareness of infection risk, and thus he/she may not be infected by the other disease. We investigate the effects of these two control strategies on key dynamical characteristics in the spreading processes of coinfectious diseases, such as epidemic threshold and phase transition. We develop a percolation-based framework to theoretically analyze how these control strategies affect the cooperative spreading epidemics.

In Sec. II, we describe the coinfection model on complex networks and the two control strategies. In Sec. III, we present the bond percolation theory to analyze the effects of two control strategies. In Sec. IV, we present results from extensive numerical computations to validate our theory. Conclusions and discussions are presented in Sec. V.

II. COINFECTION DISEASE MODEL AND SELF-AWARENESS CONTROL STRATEGIES

In the coinfection disease model, there are two coinfectious diseases a and b. Such two diseases, based on the SIR model, spread on an uncorrelated configuration network (UCM) with size N and degree distribution $P(k)$.[32] To simplify the theoretical framework, we ignore the degree–degree correlation of the network. At any time, each node can exist in one of the three states: susceptible(S), infected(I), and recovered(R). In the susceptible state, a node is susceptible and has not been infected. In the infected state, a node is infected and can transmit the same disease to his/her neighbors. The recovered state indicates that a node has recovered from the disease and will not be infected again. As the infectious disease may cause an organic injury or a degraded immune system, the infected node with the first disease will be infected more easily by the second disease. Therefore, there are the following disease-transmission rules. We use S to represent the node that is not infected by any disease (a or b). He/she is infected by its infectious neighbor with disease $a(b)$ by transition rate $\lambda_a(\lambda_b)$. Once a node has been infected by one disease (regardless of whether it is in the infected state or the recovered state), the transmission rate of the second disease becomes α ($\alpha \geq 1$) times of the original rate. α represents the synergy effect of coinfection. For example, if a node was infected with disease a and is in a recovered state of disease a, a neighboring node with disease b will infect this node with the transmission rate $\alpha\lambda_b$.

Figure 1 shows an example of a transmission process of coinfectious diseases. Initially, two randomly chosen nodes are seeds with disease a or b, respectively. If a node is infected with the disease $a(b)$, it will be in the state "a" ("b"). Under rate γ, this node becomes recovered "A" ("B") for the disease $a(b)$. Note that this recovered state is only for the disease it was infected. Here, we set the recovery rate as $\gamma = 1$ for simplicity. As shown in Fig. 1, "Ab" indicates that the node that has recovered from disease a and is currently infected with the disease b; "aB" indicates that the node that has recovered from disease b and is currently infected with the disease a; "ab" represents that the node is in the infected state with both diseases of a and b; "AB" indicates that the node has recovered from both diseases.

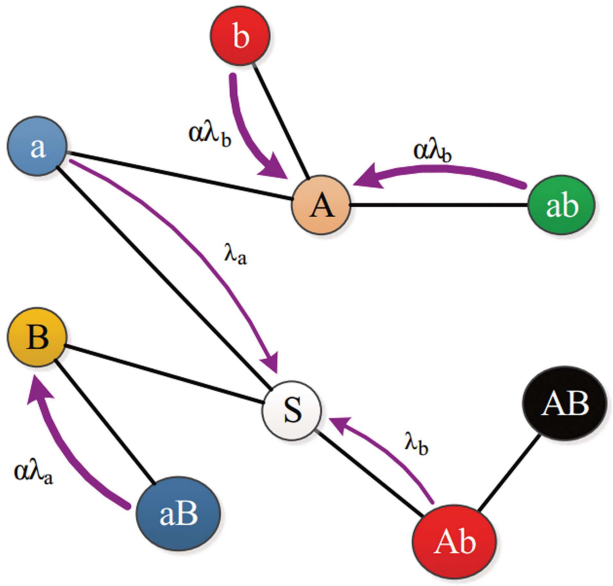

FIG. 1. Illustration of cooperative spreading processes on a network. The states of nodes are marked with letters. "*S*" indicates that a node is susceptible and has not been infected. "*a*" and "*b*" mean that a node is only infected with disease *a* or *b*. "*A*" and "*B*" represent a node that had been infected with the disease *a* or *b* and has recovered, but it is susceptible to another disease and there will be a synergistic effect. "*Ab*" indicates that the node has recovered from disease *a*, and is currently infected with the disease *b*; "*aB*" indicates that the node that has recovered from disease *b*, and is currently infected with the disease *a*; "*ab*" represents that the node is in the infected state with both diseases of *a* and *b*; "*AB*" indicates that the node has been recovered from both diseases. Black edges indicate network edges, thin purple edges indicate a normal transmission process with probability λ_a or λ_b, and coarse purple edges indicate that there is a coinfection with the synergy factor.

Two self-awareness control strategies, i.e., the immunization strategy and the quarantine strategy, are then introduced for suppressing the cooperative epidemics. In these strategies, a node infected with one disease will be immunized or quarantined based on self-awareness of infection risk, and thus he/she cannot be infected by the other disease. The difference is that the immunized node can transmit the disease it is infected, but the quarantined node cannot transmit the disease it is infected, as it cannot contact with any neighboring node.

III. THEORY

In this section, we use bond percolation theory to formalize a theoretical framework for analyzing the cooperative epidemics under the self-awareness control strategies. Based on the general theoretical framework, we deduce the epidemic thresholds of coinfectious diseases and unveil the effects of key factors such as the synergistic effect, self-awareness control strategies, and network structure on the epidemic threshold and the outbreak size. Further, we show a specific case of the general theoretical framework for the Erdős–Rényi (ER) networks.[33]

A. General theoretical framework

We begin with the case of cooperative epidemics without the control strategy. The SIR spreading can be mapped to the bond percolation process.[34] Since two diseases cooperatively spread on a single network in the coinfection disease model, the underlying network can be regarded as a double-layer coupled network with layers A_0 and B_0 whose structures are exactly the same and completely overlapping. The multiplex networks here refer to the networks with one-to-one coupling of nodes in two layers.[35] That is, a node v_{A_0} in the network A_0 only is matched with a node v_{B_0} in the network B_0, and node v_{B_0} is only matched with the node v_{A_0}. One disease $a(b)$ can only spread on one network layer $A_0(B_0)$. The interlayer edge reflects the relationship between the node v_{A_0} and v_{B_0} and will cause the synergy effects.

We consider an uncorrelated configuration network model of size N. As $N \to \infty$, the network has a tree structure with no loop and no degree correlation. In order to get the number of the nodes that is infected with two diseases, in other words, to get the size of the mutual connected giant cluster in the multiplex networks, we developed the bond percolation theory. Define x_a as the probability that one end node v_{A_0} of a randomly chosen link connects to the giant component of layer A_0. We take disease a as an example to compute this probability. The self-consistent equation for x_a can be written as

$$\begin{aligned} x_a = \sum_{k_1}\sum_{k_2} \frac{k_1 P(k_1,k_2)}{\langle k_1\rangle} \Big\{ & p[1-(1-\alpha\lambda_a x_a)^{k_1-1}] \\ & \times [1-(1-\lambda_b x_b)^{k_2}] + (1-p)[1-(1-\lambda_a x_a)^{k_1-1}] \\ & \times [1-(1-\alpha\lambda_b x_b)^{k_2}] \\ & + [1-(1-\lambda_a x_a)^{k_1-1}](1-\lambda_b x_b)^{k_2} \Big\}, \end{aligned} \tag{1}$$

where $P(k_1,k_2)$ is the joint probability that node v_{A_0} in A_0 and its counterpart v_{B_0} in B_0 have degree of k_1 and k_2, respectively. According to the coinfection mechanism, if a node is in the giant component of layer A_0, it would be in AB state or A state ultimately. If the node v_{A_0} is infected with two diseases (i.e., in the AB state), there will be two possible infection pathways. The first right-hand term of Eq. (1) represents the first pathway. Specifically, its counterpart v_{B_0} is first infected by disease b with probability $1-(1-\lambda_b x_b)^{k_2}$, and then the node v_{A_0} is infected by disease a with probability $1-(1-\alpha\lambda_a x_a)^{k_1-1}$, where α represents the synergistic effect of coinfection and k_1-1 indicates the neighboring number of node v_{A_0} except the first chosen one. The second pathway is described by the second right-hand term of Eq. (1). In this case, node v_{A_0} is first infected by disease a with probability $1-(1-\lambda_a x_a)^{k_1-1}$, and then the synergistic effect affects the infection of disease b on layer B_0 with probability $1-(1-\alpha\lambda_b x_b)^{k_2}$. If node v_{A_0} was only infected with disease a (i.e., A state), and its counterpart v_{B_0} does not be infected by the disease b on layer B_0, it is represented as the third right-hand term of Eq. (1). Since the bond percolation corresponds to the long-term behavior of the SIR model, it cannot describe the time evolution of SIR spreading and the infection order of two diseases. Here, we denote p as the probability that a node is infected by the disease b firstly and then by the disease a in a statistical sense. The value of p relates to factors such as the network structure and the disease transmission rate.

Since layers A_0 and B_0 are exactly the same and completely overlapping, there are perfect interlayer degree correlations between two layers. We can get $P(k_1, k_2) = P(k)$ if $k_1 = k_2 = k$; else $P(k_1, k_2) = 0$. So Eq. (1) is transformed into

$$\begin{aligned} x_a = \sum_k \frac{kP(k)}{\langle k\rangle} \Big\{ & p[1-(1-\alpha\lambda_a x_a)^{k-1}][1-(1-\lambda_b x_b)^k] \\ & + (1-p)[1-(1-\lambda_a x_a)^{k-1}][1-(1-\alpha\lambda_b x_b)^k] \\ & + [1-(1-\lambda_a x_a)^{k-1}](1-\lambda_b x_b)^k \Big\}, \end{aligned} \tag{2}$$

where $kP(k)/\langle k\rangle$ is the probability that a randomly chosen edge connects to a node with degree k.

Next, we consider the effects of self-awareness control strategies. In the immunization strategy, the immunized node can transmit the disease it is infected but will not be infected by or transmits the other disease. In the quarantine strategy, the quarantined node will not transmit the disease it is infected nor be infected by the other disease. Denoting the control rate as q, the self-consistent equation for x_a can be written as

$$\begin{aligned} x_a = \sum_k \frac{kP(k)}{\langle k\rangle} \Big\{ & \Big\{ p[1-(1-\alpha\lambda_a x_a)^{k-1}][1-(1-\lambda_b x_b)^k] \\ & + (1-p)[1-(1-\lambda_a x_a)^{k-1}][1-(1-\alpha\lambda_b x_b)^k] \Big\}(1-q)^C \\ & + [1-(1-\lambda_a x_a)^{k-1}](1-\lambda_b x_b)^k (1-q)^{C-1} \Big\}. \end{aligned} \tag{3}$$

In Eq. (3), $q = 0$ corresponds to the original case of coinfection where there is no control strategy. When $q \neq 0$ and $C = 1$, the effect of immunization strategy is captured. If the node v_{A_0} was infected with two diseases (i.e., AB state), it should be unimmunized for the first-infected disease with probability $(1-q)$, corresponding to the first two items of Eq. (3). If the node v_{A_0} is only infected with the disease a, it makes no difference with the case when no self-awareness control strategy is used, as indicated in the last term of Eq. (3). When $q \neq 0$ and $C = 2$, it is the case of quarantine strategy. In this strategy, a node infected with disease a will lose the chance to transmit disease a and cannot be infected by the disease b thus it is unimmunized for both disease with probability $(1-q)^2$, corresponding to the first two items of Eq. (3). Since a node v_{A_0} infected with the disease a is removed because of self-awareness quarantine, the node is unimmunized for disease a with probability $1-q$, corresponding to the last term of Eq. (3).

Analogously, we can get the self-consistent equation for x_b. Using the generating function and merging x_a and x_b, we can transform the expressions of $x_i (i = a, b)$ into

$$\begin{aligned} x_i = (1-q)^C \Big\{ & p\Big\{ 1 - G_1(1-\alpha\lambda_a x_a) + (1-\lambda_b x_b) \\ & \times [G_1((1-\lambda_a x_a)(1-\alpha\lambda_b x_b)) - G_1(1-\alpha\lambda_b x_b)] \Big\} \\ & + (1-p)\Big\{ 1 - G_1(1-\lambda_a x_a) + (1-\alpha\lambda_b x_b) \\ & \times [G_1((1-\lambda_a x_a)(1-\alpha\lambda_b x_b)) - G_1(1-\alpha\lambda_b x_b)] \Big\} \Big\} \\ & + [G_1(1-\lambda_j x_j) - G_1((1-\lambda_i x_i)(1-\lambda_j x_j))] \\ & \times (1-\lambda_j x_j)(1-q)^{C-1}. \end{aligned} \tag{4}$$

In Eq. (4), when x_i is x_a, x_j is x_b and vice versa, λ_i is the propagation rate of disease i. $G_1(x) \equiv \sum_k \frac{kP(k)}{\langle k\rangle} x^{k-1}$ is the generating function for the excess degree distribution. Once the probabilities x_a and x_b are obtained, we can get the concurrent outbreak size of two diseases P_{ab}, thus the size of the giant coinfected cluster, by calculating

$$\begin{aligned} P_{ab} = \sum_k P(k) \Big\{ & p[1-(1-\alpha\lambda_a x_a)^k][1-(1-\lambda_b x_b)^k] \\ & + (1-p)[1-(1-\lambda_a x_a)^k][1-(1-\alpha\lambda_b x_b)^k] \Big\}(1-q)^C. \end{aligned} \tag{5}$$

Using the generating function, we can transform Eq. (5) into

$$\begin{aligned} P_{ab} = \Big\{ & p[1-G_0(1-\alpha\lambda_a x_a) - G_0(1-\lambda_b x_b) \\ & + G_0((1-\alpha\lambda_a x_a)(1-\lambda_b x_b))] \\ & + (1-p)[1-G_0(1-\lambda_a x_a) - G_0(1-\alpha\lambda_b x_b) \\ & + G_0((1-\lambda_a x_a)(1-\alpha\lambda_b x_b))] \Big\}(1-q)^C, \end{aligned} \tag{6}$$

in which $G_0(x) \equiv \sum_k P(k)x^k$ is the generating function for the degree distribution. For a given network of arbitrary degree distribution and control strategy, the final concurrent outbreak size of the two diseases can be obtained from Eqs. (4) and (6).

The epidemic threshold is another important parameter in spreading dynamics. Taking disease a for example, in the bond percolation theory, Eq. (4) has a trivial solution of $x_a = 0$. When there is a nontrivial stable solution, the disease is in an outbreak state. The epidemic threshold is obtained by solving the nontrivial solution of Eq. (4). For network of arbitrary degree distribution, to determine λ_c^I, the discontinuous transition threshold of disease a, we first rewrite Eq. (4) to be

$$x_a = f_a(\lambda_a, x_a, x_b). \tag{7}$$

Similarly, we can write the equation

$$x_b = f_b(\lambda_a, x_a, x_b), \tag{8}$$

where $f_i(\lambda_a, x_a, x_b)$ is the right-hand side of Eq. (4). At the critical point λ_c^I, the condition

$$\frac{\partial f_a(\lambda_c^I, x_a, x_b)}{\partial x_b} \frac{\partial f_b(\lambda_c^I, x_a, x_b)}{\partial x_a} = 1 \tag{9}$$

is fulfilled.

For the continuous phase transition of disease a, $x_a = 0$ at the critical point λ_c^{II}. This means when $\lambda_a \to \lambda_c^{II}$, we have $x_a \to 0$. Note

that it does not imply $x_b \to 0$. Actually, when $x_a \to 0$, we have

$$x_b = (1-q)^{c-1} \cdot [G_1(1) - G_1(1-\lambda_b x_b)]. \tag{10}$$

Usually for the more general cases, we could numerically get the solution of x_b by iterative calculations starting from a value close to 1. Submitting x_b to Eq. (7) and when $x_a \to 0$, we have

$$1 = \frac{\partial f_a(\lambda_c^{II}, x_a, x_b)}{\partial x_a}\Big|_{x_a=0}. \tag{11}$$

We can solve Eq. (11) to get the λ_c^{II}. Similarly, for disease b, we can use the same method to get the continuous threshold and discontinuous threshold.

B. The analysis of phase transition without control strategies

To describe how to calculate the epidemic threshold in detail, we first apply the general theoretical framework to analyze phase transition without control strategies when $q = 0$. We assume that the network is an ER random graph, then $G_0(x) = G_1(x) = e^{-<k>(1-x)}$. Assuming that both diseases have the same transmission rate, that is, $\lambda_a = \lambda_b = \lambda$, we have $x_a = x_b = x$, $p = 1/2$. Equation (4) can thus be rewritten as

$$\begin{aligned} x = {} & p[1 - e^{-\alpha\langle k\rangle\lambda x} + (1-\lambda x)(e^{\langle k\rangle\lambda x(\alpha\lambda x-1-\alpha)} - e^{-\langle k\rangle\lambda x})] \\ & + (1-p)[1 - e^{-\langle k\rangle\lambda x} + (1-\alpha\lambda x)(e^{\langle k\rangle\lambda x(\alpha\lambda x-1-\alpha)} - e^{-\langle k\rangle\alpha\lambda x})] \\ & + (1-\lambda x)(e^{-\langle k\rangle\lambda x} - e^{\langle k\rangle\lambda x(\lambda x-2)}). \end{aligned} \tag{12}$$

The critical point can be obtained from Eqs. (9) and (11). For ER networks, Eq. (12) has a trivial solution $x = 0$. When $\alpha = 1$, at the critical point, the function $F(x, \lambda, \alpha) = f(x) - x$ is tangent to the horizontal axis at $x = 0$, that is, $f'(x) = 1$ at $x = 0$. We can get the continuous critical transmission rate as

$$\lambda_c^{II} = \frac{1}{\langle k\rangle}, \tag{13}$$

which has the same form as the epidemic threshold of the SIR model.

When $\alpha > 1$, $F(x, \lambda, \alpha)$ is affected by the synergy factor α and may not be tangent to the horizontal axis at $x = 0$. It is thus reasonable to focus on how synergy factor affects the dependence of the final infected cluster size of two diseases P_{ab} on the transmission rate λ, which can be obtained from the solutions of Eq. (12). We are particularly interested in finding out whether the dependence is continuous or discontinuous. Note that Eq. (12) always has a trivial solution $x = 0$. As shown in Figs. 2(a) and 2(b), numerical results indicate that the number of roots can be 1, 2, or 3. When we fix all the parameters except λ, if Eq. (12) has one root or two roots for different values of λ (see Fig. 2), P_{ab} will increase continuously with λ. For the case of one root $x = 0$, two diseases cannot spread out. If the number of roots of Eq. (12) is 2 or 3, as shown in Fig. 2(b), saddle-node bifurcation occurs. The saddle-node bifurcation occurs because there is only one stable solution of $x = 0$ before tangent bifurcation, and with the increase of λ two stable solutions of $x = 0$ and $x \neq 0$ (the larger solution) will appear after tangent. The bifurcation of Eq. (12) reveals that the system undergoes a cusp catastrophe: Varying λ, the physically meaningful stable solution of x will suddenly jump to a large value. In this case, a discontinuous growth pattern of P_{ab} with λ emerges, and the critical transmission rate λ_c^I at which the discontinuity occurs can be obtained by solving Eqs. (4) and (9). We propose an example of $\alpha = 3$ to explain the phenomenon that P_{ab} increases discontinuously with λ. As shown in Fig. 2(b), the function $F(x, \lambda, \alpha)$ is tangent to the horizontal axis at $\lambda_c^I \approx 0.084$. When $\lambda < \lambda_c^I$, Eq. (4) has one fixed point of $x = 0$, indicating that the two diseases cannot encounter with each other. When $\lambda = \lambda_c^I$, a new solution is given by the tangent point. When $\lambda > \lambda_c^I$, if Eq. (4) has two fixed points except $x = 0$, then the solution will be given by the largest one (since only this root is stable). In this case, the stable solution of Eq. (12) changes from a relatively small value near $\lambda = \lambda_c^I$ to a large value abruptly, leading to a discontinuous change in P_{ab} .

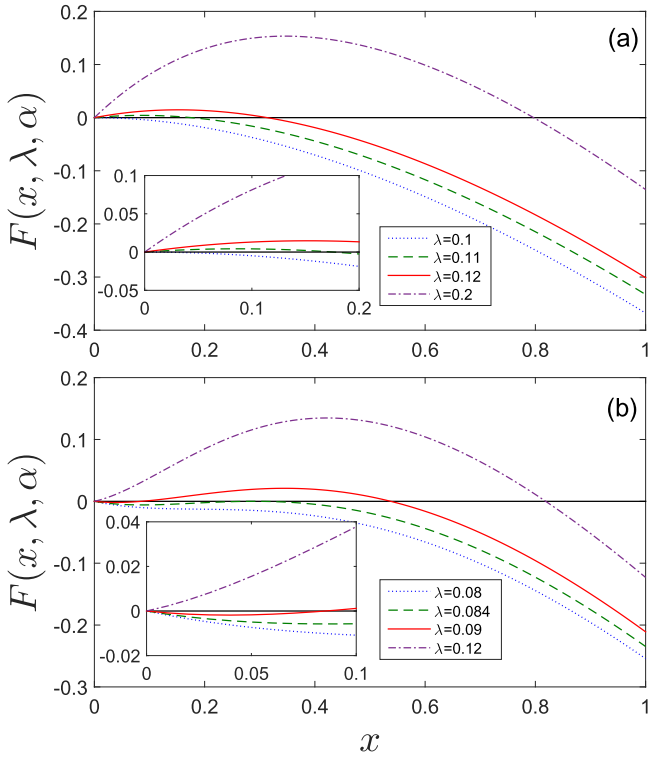

FIG. 2. Diagram of Eq. (12). For ER random networks, (a) when $\alpha = 1$, P_{ab} increases continuously with λ. Equation (12) has one root or two roots for different values of λ. (b) When $\alpha = 3$, P_{ab} increases discontinuously with λ. The number of roots of Eq. (12) depends on λ. In order to show the number of roots clearly, the subfigures are the front part of the large images. Mean degree $\langle k\rangle$ is set to be 10.

When $\alpha = 3$, the critical transmission rate λ_c^I is smaller than λ_c^{II} which corresponds to $\alpha = 1$. That is, the critical transmission rate can be reduced by increasing the synergy factor. This is because when α is small, such as $\alpha = 1$, there is little synergy effects. In order to get a certain proportion of nodes infected with two diseases, the two diseases need a large number of nodes infected the disease a or b, respectively, thus the λ_c is large. When α is large, such as $\alpha = 3$, there is a synergistic effect. The transmission of the two diseases enhance each other mutually, and a certain proportion of nodes infected with

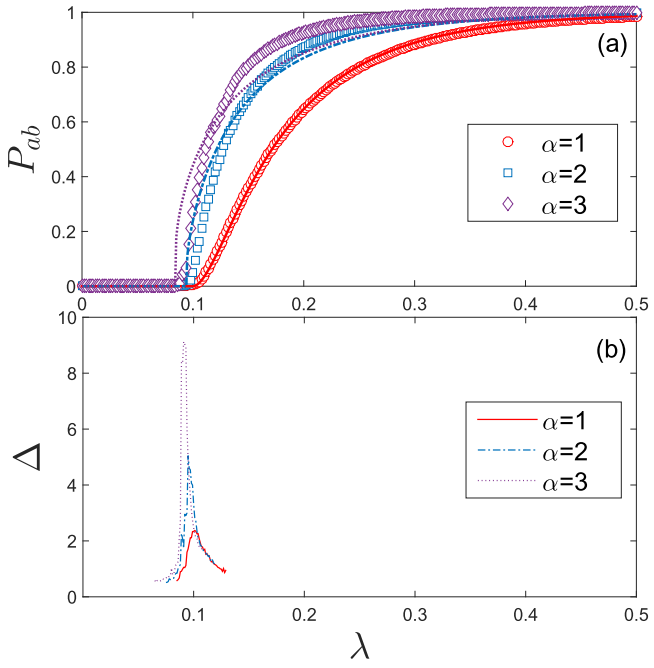

FIG. 3. The co-infected outbreak size of ER random networks. (a) In the final state, the proportion of nodes that ultimately are infected by both diseases P_{ab} varies with the transmission rate λ for the synergy factor $\alpha = 1$ (red circles), $\alpha = 2$ (blue squares), and $\alpha = 3$ (purple diamonds). (b) Variability changes with transmission rate λ for synergy factor $\alpha = 1$ (red solid line), $\alpha = 2$ (blue dotted dashed line), $\alpha = 3$ (purple dotted line). The lines in (a) is obtained by solving Eqs. (4) and (6).

two diseases can be produced when they are in contact with each other. The two diseases need a small range of infections, respectively, thus the λ_c decreases.

To determine the critical parameter of α_s, at which the dependence of P_{ab} on λ changes from being continuous to discontinuous, we have the condition[36]

$$\frac{\partial^2 f_a(\lambda, x_a, x_b)}{\partial x_b^2} = 0, \quad \frac{\partial^2 f_b(\lambda, x_a, x_b)}{\partial x_a^2} = 0. \tag{14}$$

For a fixed network structure, the critical values of the system parameters λ_c and α_s can be determined.

C. The analysis of phase transition under two self-awareness strategies

Then, we consider phase transition under two self-awareness strategies. We analyze the case of $q \neq 0$, $C = 1$, representing the effects of immunization strategy on ER networks. The critical condition can be obtained from Eqs. (9) and (11). For the ER random networks, Eq. (4) has a trivial solution of $x = 0$. When $\alpha = 1$, we can get the critical transmission rate $\lambda_c^{II} = 1/\langle k \rangle$, which is the same as that without the immunization strategy. This is because when $\alpha = 1$, there is no cooperation between the two diseases and the epidemics of two diseases are the same as the original SIR model. Since

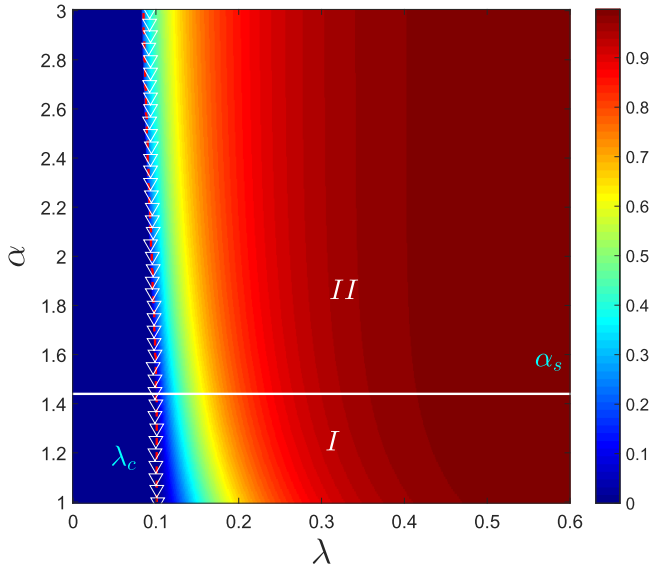

FIG. 4. P_{ab} changes in the parameter plane (λ, α). The illustration is obtained by solving Eqs. (4) and (6). The red dashed line indicates the theoretical thresholds and the white inverted triangles are the numerical thresholds obtained by the peak of variability. The white solid line is the threshold of synergy factor $\alpha_s \approx 1.44$, obtained by solving Eq. (14). On the sides of the synergy threshold, there is a continuous phase transition in the *I* region, while a discontinuous phase transition in the *II* region.

the immunized node is immunized to the second disease, it cannot spread it. Thus, the propagation threshold does not change under the immunization strategy. However, when $\alpha > 1$, $F(x, \lambda, \alpha)$ is affected by the synergy factor α and may be not tangent to the horizontal axis at $x = 0$. In this case, a saddle-node bifurcation occurs and the propagation threshold changes.

To determine the critical synergy factor α_s, the condition of Eq. (14) must be established. When $\alpha < \alpha_s$, there is no discontinuous phase transition and when $\alpha \geq \alpha_s$, there is a discontinuous phase transition at $\lambda = \lambda_c^I$. We can numerically solve Eqs. (4), (9), and (14) to get α_s under the immunization strategy. When fixing the synergy factor $\alpha \geq \alpha_s$, we can get the other critical parameter

$$q_s = 1 - \frac{1 - \lambda_c(1 - \lambda_c x)[G_1(1 - \lambda_c x) - G_1((1 - \lambda_c x)(1 - \lambda_c x))]}{\lambda_c M} \tag{15}$$

by Eqs. (4), (9), and (14), where

$$M = \alpha p[G_1'(1 - \alpha\lambda_c x) - (1 - \lambda_c x)^2 G_1'((1 - \alpha\lambda_c x)(1 - \lambda_c x))] + (1-p)[G_1'(1-\lambda_c x) - (1-\alpha\lambda_c x)^2 G_1'((1 - \lambda_c x)(1 - \alpha\lambda_c x))]. \tag{16}$$

The q_s is the critical immunization rate. When $q < q_s$, it is a discontinuous phase transition and when $q \geq q_s$, it is continuous. For a fixed network structure, the critical values of the system parameters λ_c, α_s, and $q_s$can be determined under the immunization strategy.

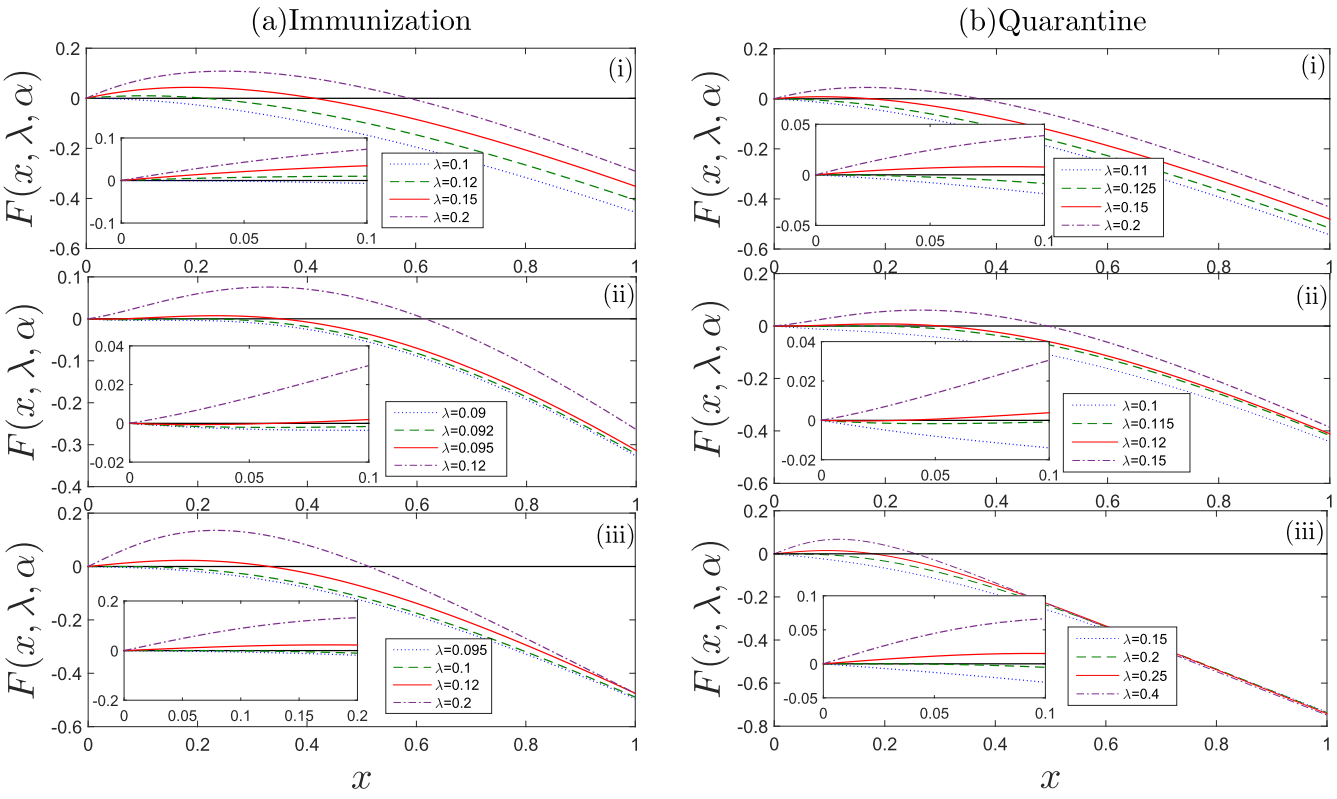

FIG. 5. Diagram of Eq. (4) for $C = 1$ and $C = 2$. (a) The effects of immunization strategy on ER networks with $C = 1$. (i) When $\alpha = 1$, $q = 0.2$, P_{ab} increases continuously with growing of λ. Equation (4) has one root or two roots for different values of λ and the parameter q has no effect on the epidemic threshold. (ii) When $\alpha = 3$, $q = 0.2$, P_{ab} increases discontinuously with the growing of λ. The number of roots of Eq. (4) depends on λ and saddle-node bifurcation occurs. (iii) When $\alpha = 3$, $q = 0.5$, P_{ab} increases continuously with the growing of λ. Equation (4) has one root or two roots for different values of λ again. (b) The effects of quarantine strategy on ER networks with $C = 2$. (i) When $\alpha = 1$, $q = 0.2$, P_{ab} increases continuously with growing of λ. (ii) When $\alpha = 3$, $q = 0.2$, P_{ab} increases discontinuously with growing of λ. (iii) When $\alpha = 3$, $q = 0.5$, P_{ab} increases continuously with growing of λ. The black line represents the horizontal axis. In order to show the number of root clearly, the subfigures are the front part of the larger images.

Finally, we investigate the effects of quarantine strategy with $q \neq 0$ and $C = 2$. Equation (4) has a trivial solution of $x = 0$ for the ER random networks. When $\alpha = 1$, we can get the critical transmission rate

$$\lambda_c^{II} = \frac{1}{(1-q)\langle k\rangle}. \tag{17}$$

It indicates that when $\alpha = 1$, the quarantine strategy can increase the epidemic threshold. When $\alpha > 1$, $F(x,\lambda,\alpha)$ is affected by the synergy factor α and may be not tangent to the horizontal axis at $x = 0$.

We can also numerically solve Eqs. (4), (9), and (14) to get α_s under the quarantine strategy. When fixing synergy factor $\alpha \geq \alpha_s$, we can get the critical parameter

$$q_s = 1 - \frac{1}{\lambda_c M(1-q_s)} - \frac{(1-\lambda_c x)[G_1(1-\lambda_c x) - G_1((1-\lambda_c x)(1-\lambda_c x))]}{M}, \tag{18}$$

where M is defined in Eq. (16). For a fixed network structure, the critical values of the system parameters λ_c, α_c, and q_s can be determined under the quarantine strategy.

IV. NUMERICAL VERIFICATION

We perform extensive simulations of cooperative epidemics on ER networks[33] and configuration networks with power-law degree distribution,[37] where the network size and mean degree are $N = 10^4$ and $\langle k\rangle = 10$, respectively. Simulations are performed on at least 100 networks and on each network, 2×10^3 independent dynamical realizations are performed to calculate the average values. We separately discuss the effects of synergy mechanism and control strategy on cooperative epidemics.

A. The effect of synergy mechanism

We first study how synergy mechanism influences the spreading dynamics on the ER random networks without control strategy.

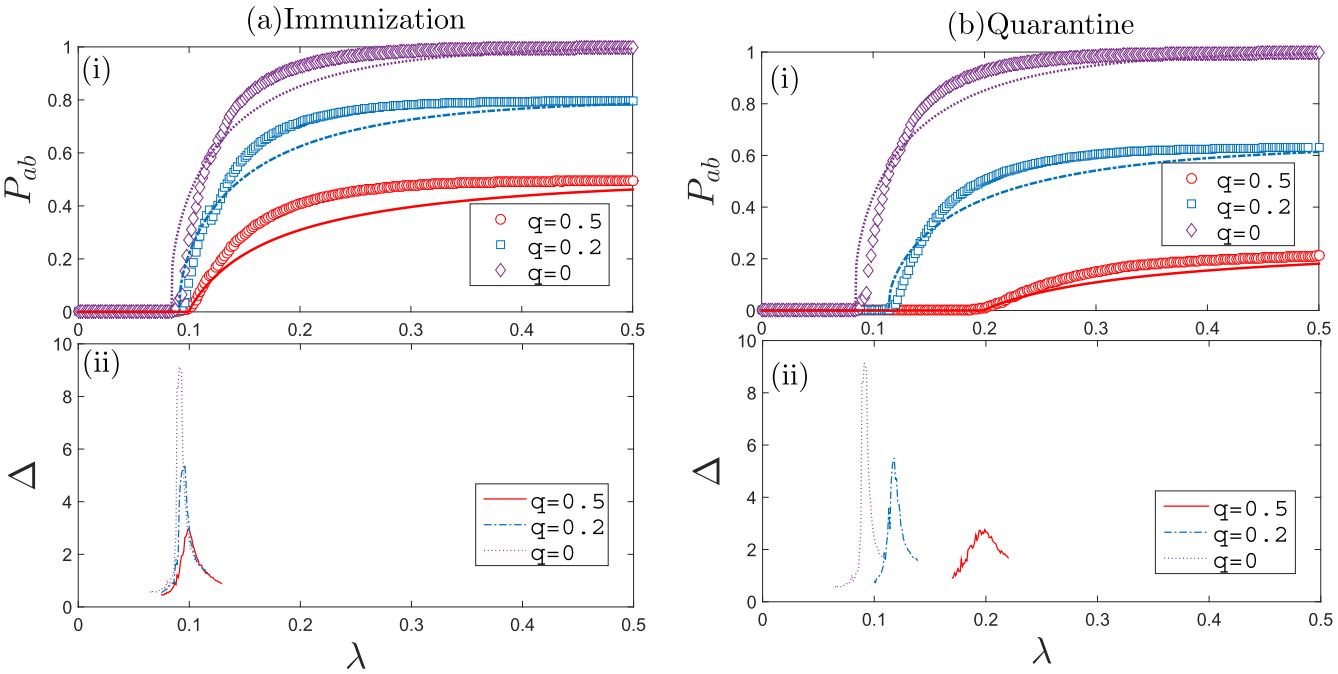

FIG. 6. Cooperative epidemics on ER random networks under immunization strategy (a) and quarantine strategy (b). In both (a) and (b), (i) the proportion of nodes that ultimately are infected with both diseases P_{ab} varies with the transmission rate λ under the immunization rates $q = 0.5$ (red circles), $q = 0.2$ (blue squares), and $q = 0$ (purple diamonds). (ii) Variability as a function of transmission rate λ at immunization rates $q = 0.5$ (red solid line), $q = 0.2$ (blue dotted-dashed line), $q = 0$ (purple dotted line). And the lines in (i) is obtained by solving Eqs. (4) and (6).

The parameters are set as$q = 0$, $\lambda_a = \lambda_b = \lambda$. We focus on the proportion of nodes that are infected by two diseases P_{ab} as a function of the transmission rate λ for different synergy factor α. As shown in Fig. 3(a), with the increase of α, the epidemic threshold decreases and the final coinfected size increases. The type of phase transition transforms from being continuous to discontinuous. When there is no synergy effect, i.e., synergy factor $\alpha = 1$, P_{ab} increases continuously with the transmission rate λ, which is the same as the classical SIR model. As α increases to $\alpha = 3$, P_{ab} increases discontinuously with λ, since the synergy effect enhances the spread of the other disease. The theoretical value of λ_c can be solved by Eqs. (4), (9), and (11) and simulated epidemic threshold can be identified by the peak of variability.[38,39] The variability can be calculated as

$$\Delta = \frac{\sqrt{\langle P_{ab}^2 \rangle - \langle P_{ab} \rangle^2}}{\langle P_{ab} \rangle}. \tag{19}$$

As shown in Fig. 3(b), there is a peak of variability at λ_c^I ($\alpha = 2, 3$) and λ_c^{II} ($\alpha = 1$), where $\lambda_c^{II} \approx 0.101$ for $\alpha = 1$, $\lambda_c^I \approx 0.095$ for $\alpha = 2$, and $\lambda_c^I \approx 0.091$ for $\alpha = 3$ obtained by simulation of epidemic dynamics.

We try to explain the above crossover phenomenon of phase transition. Research studies on cooperative epidemics show that before the two diseases meet, they spread in a certain range.[16,17] When the two diseases meet, the node originally infected with one disease, no matter it is in I or R state for the disease, will be infected by the other one. Thus, a certain range of coinfection nodes may appear immediately. The infected ranges of a single disease are different on different networks. On the two-dimensional lattice, two kinds of diseases will meet each other quickly because of few paths between nodes, and the number of coinfection nodes thus continuously increases with the transmission rate. On the ER random networks, there are many propagation paths among nodes. When two diseases meet, if the synergy factor α is small, such as $\alpha = 1$, the encounter of the two diseases does not promote the coinfection of nodes as the synergy does not work. Thus, the phase transition is still continuous. If the synergy factor α is large, such as $\alpha = 3$, the synergy effect enhances the spread of the other disease, and a large number of coinfection nodes suddenly appear resulting in a discontinuous phase transition.

Next, we investigate the relations of the transmission rate λ, the synergy factor α, and the proportion of coinfection nodes P_{ab}, as shown in Fig. 4. The illustration is obtained by solving Eqs. (4) and (6). The red dashed line represents the theoretical thresholds derived from Eqs. (4), (9), and (11) and the white inverted triangles are the numerical thresholds, obtained by the peak of variability. The white solid line is the critical synergy factor $\alpha_s \approx 1.44$, obtained by solving Eqs. (4), (9), and (14). On the sides of solid line, the I region is a continuous phase transition and the II is a discontinuous phase transition. It can be seen clearly that with the increase of the synergy factor α, the threshold of cooperative epidemics is reduced. That implies the synergistic effect makes the disease easier to spread.

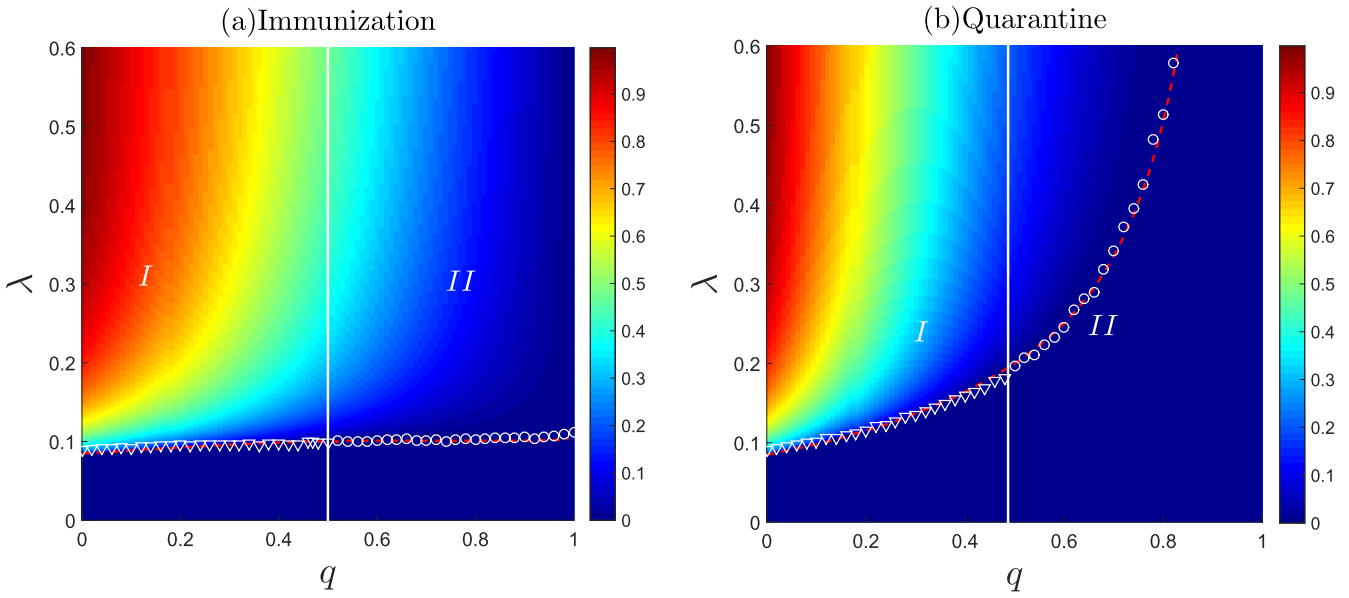

FIG. 7. P_{ab} varies with (q, λ). In immunization strategy (a) and quarantine strategy (b), the illustration is obtained by solving Eqs. (4) and (6). The red dashed line is the theoretical thresholds and the white inverted triangle and white circle are the numerical thresholds obtained by the peak of variability. Note that the white inverted triangle are discontinuous thresholds and the white circle are continuous thresholds. White solid line in figure (a) is the critical immunization rate $q_s \approx 0.5$, obtained by solving Eq. (15). The white solid line in figure (b) is the critical quarantine rate $q_s \approx 0.487$, obtained by solving Eq. (18). On the sides of the q_s, the *I* region is a discontinuous phase transition and the *II* is a continuous phase transition.

B. The effect of control strategy

In this section, we study the effects of control strategies on the cooperative epidemics on ER random networks. Similarly, we set $\lambda_a = \lambda_b = \lambda$. We first theoretically analyze the influence of the immunization/quarantine rate on the epidemic threshold. For the immunization strategy, $q \neq 0$ and $C = 1$ in Eq. (4). When $\alpha = 1$, $q = 0.2$ as shown in Fig. 5(a)(i), Eq. (4) has one root or two roots for different values of λ. This means that P_{ab} increases continuously with λ. $F(x, \lambda, \alpha)$ is tangent to the horizontal axis at $\lambda_c^{II} \approx 0.1$, which is the same as $\alpha = 1$, $q = 0$ in Fig. 2(a), indicating that the immunization rate q does not affect the epidemic threshold in this case. When $\alpha = 3$, $q = 0.2$, as shown in Fig. 5(a)(ii), the number of roots of Eq. (4) depends on λ and saddle-node bifurcation occurs. This means that P_{ab} increases discontinuously with λ. $F(x, \lambda, \alpha)$ is tangent to the horizontal axis at $\lambda_c^{I} \approx 0.092$. The immunization strategy increases the epidemic threshold compared with the case of $\alpha = 3$ and $q = 0$ as shown in Fig. 2(b), while the type of phase transition remains discontinuous. When $\alpha = 3$, $q = 0.5$, as shown in Fig. 5(a)(iii), Eq. (4) has one root or two roots for different values of λ, and thus P_{ab} increases continuously with λ. $F(x, \lambda, \alpha)$ is tangent to the horizontal axis at $\lambda_c^{II} \approx 0.1$. This means that with the increase of the immunization rate, not only the propagation threshold increases, but also the type of phase transition changes from being discontinuous to continuous. When the immunization rate grows, the intersection of $F(x, \lambda, \alpha)$ and the horizontal axis becomes smaller, implying that the epidemic spreading is suppressed.

For quarantine strategy, $q \neq 0$ and $C = 2$ in Eq. (4). When $\alpha = 1$, $q = 0.2$ as shown in Fig. 5(b)(i), Eq. (4) has one root or two roots for different values of λ. $F(x, \lambda, \alpha)$ is tangent to the horizontal axis at $\lambda_c^{II} \approx 0.125$, which is different from the case of $\alpha = 1$ and $q = 0$ as shown in Fig. 2(a), indicating that the quarantine strategy enhances the epidemic threshold, but the type of phase transition remains continuous. When $\alpha = 3, q = 0.2$, as shown in Fig. 5(b)(ii), saddle-node bifurcation occurs, and $F(x, \lambda, \alpha)$ is tangent to the horizontal axis at $\lambda_c^{I} \approx 0.115$. The quarantine strategy increases the epidemic threshold, while the type of phase transition is still discontinuous. When $\alpha = 3$, $q = 0.5$, as shown in Fig. 5(iii), Eq. (4) has one root or two roots for different values of λ, and $F(x, \lambda, \alpha)$ is tangent to the horizontal axis at $\lambda_c^{II} \approx 0.2$. This implies that the epidemic threshold increases with the quarantine rate, and the type of phase transition changes from being discontinuous to continuous. Comparing Figs. 5(a) and 5(b), we can see that the quarantine strategy has a better effect in suppressing the discontinuous phase transition and reducing the outbreak size than the immunization strategy.

Next, we investigate the effects of different control strategies on the outbreak size of cooperative epidemics. Figure 6 shows the proportion of nodes infected with both diseases P_{ab} as a function of transmission rate λ under different control rates when $\alpha = 3$. For immunization strategy, as shown in Fig. 6(a)(i), with the increase of immunization rate q, the epidemic threshold increases, the outbreak size decreases, and the type of phase transition transforms from being discontinuous to continuous. When $q = 0$, P_{ab} increases discontinuously with λ, which is the same case as Fig. 3. As q increases to 0.5, P_{ab} increases continuously with λ. In Fig. 6(a)(ii), the peak

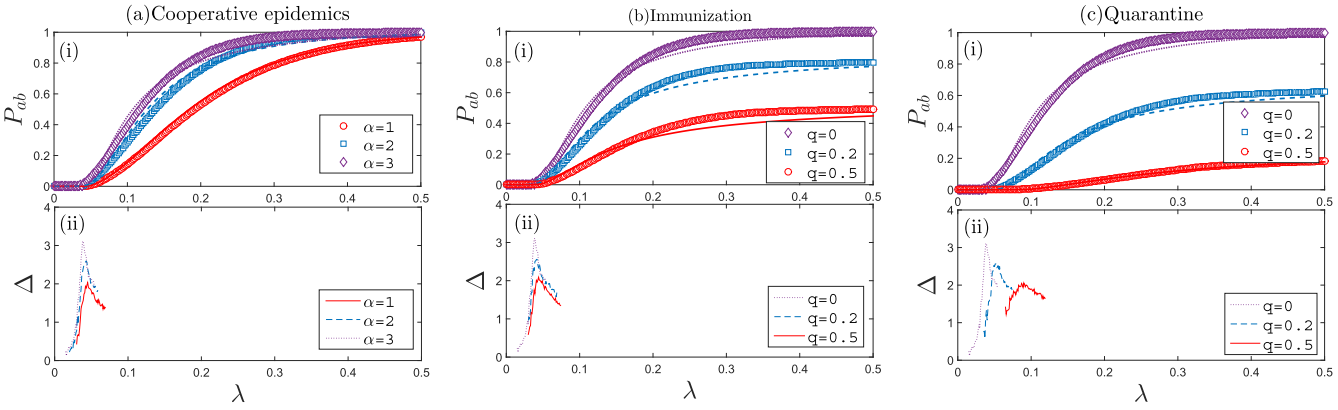

FIG. 8. The impacts of synergistic effect and control strategies on cooperative epidemics on scale-free networks. (a) Cooperative epidemics. (i) P_{ab} varies with λ under the synergy factors $\alpha = 1$ (red circles), $\alpha = 2$ (blue squares), $\alpha = 3$ (purple diamonds). (ii) Variability changes with λ at synergy factors $\alpha = 1$ (red solid line), $\alpha = 2$ (blue dotted-dashed line), $\alpha = 3$ (purple dotted line). The corresponding lines in (i) are obtained by solving Eqs. (4) and (6). (b) Immunization strategy and (c) quarantine strategy. (i) P_{ab} varies with λ under the rates $q = 0$ (purple diamonds), $q = 0.2$ (blue squares), and $q = 0.5$ (red circles). (ii) Variability changes with λ at the rates $q = 0$ (purple diamonds), $q = 0.2$ (blue squares), and $q = 0.5$ (red circles). We set the structural parameters as $\gamma = 2.7$ and $\langle k \rangle = 10$.

of variability corresponds to $\lambda_c^I \approx 0.091$ for $q = 0$, $\lambda_c^I \approx 0.096$ for $q = 0.2$, and $\lambda_c^{II} \approx 0.099$ for $q = 0.5$ obtained by simulation of epidemic dynamics. For quarantine strategy, as shown in Fig. 6(b)(i), it plays a similar effect on cooperative epidemics with the immunization strategy. From 6(b)(ii), we can see $\lambda_c^I \approx 0.091$ for $q = 0$, $\lambda_c^I \approx 0.118$ for $q = 0.2$, and $\lambda_c^{II} \approx 0.199$ for $q = 0.5$ obtained by simulation of epidemic dynamics. The existence of control strategy suppresses the discontinuous phase transition and the spread of cooperative epidemics. Comparing Fig. 6(a) with Fig. 6(b), it can be seen that the quarantine strategy is more effective than the immunization strategy, which is consistent with the theoretical results.

Figure 7 shows the relations of the transmission rate λ, the control rate and the ratio of coinfected nodes P_{ab}. For immunization strategy, in Fig. 7(a), the results are obtained by solving Eqs. (4) and (6). It can be seen that with an increase of immunization rate q, the epidemic threshold increases, implying that the immunization strategy makes the disease more difficult to spread. The white solid line is the critical immunization rate $q_s = 0.5$, obtained by solving Eq. (15). In the I region in Fig. 7(a), P_{ab} changes with λ discontinuously at the critical point, since Eq. (4) has a saddle-node bifurcation phenomenon when $0 \le q \le 0.5$. In the II region, P_{ab} changes with λ continuously, and Eq. (4) has no bifurcation when $0.5 < q \le 1$. Compared with the immunization strategy, quarantine strategy has a smaller critical control rate and a greater increase in epidemic threshold [see Fig. 7(b)], and thus has a better control effect on the cooperative epidemics.

We further construct scale-free networks based on the configuration model[37] to study the cooperative epidemics and the effects of control strategies. The degree distribution of scale-free networks follows $P(k) \sim k^{-\gamma}$, where the degree exponent, network size, and average degree are $\gamma = 2.7$, $N = 10^4$, and $\langle k \rangle = 10$. We set $\lambda_a = \lambda_b = \lambda$ and $x_a = x_b = x$, $p = 1/2$. The generating functions for the degree distribution and the excess degree distribution are $G_0(x) \equiv \sum_k P(k)x^k$ and $G_1(x) \equiv \sum_k \frac{kP(k)}{\langle k \rangle} x^{k-1}$, respectively. Due to the structural characteristics of scale-free networks, the two diseases quickly meet at the hub nodes and there is no discontinuous phase transition.[16] Fig. 8(a)(i) shows that although the synergy factor α increases, the type of phase transition remains continuous. Meanwhile, the synergistic effect enhances the spread of the other disease when two diseases meet, thus reducing the epidemic threshold and increasing the outbreak size of epidemics. Using the variability measure, we get $\lambda_c^{II} \approx 0.045$ for $\alpha = 1$, $\lambda_c^{II} \approx 0.043$ for $\alpha = 2$, and $\lambda_c^{II} \approx 0.039$ for $\alpha = 3$ obtained by simulation of epidemic dynamics, as shown in Fig. 8(a)(ii). Since the two diseases meet each other near the hubs, the increase of the synergy factor has little effect on the epidemic threshold, while the threshold decreases with the synergy factor.

When we fix the synergy factor $\alpha = 3$, for immunization strategy, it can be seen from Fig. 8(b)(i) that increasing the immunization rate can enhance epidemic threshold and reduce the outbreak size of cooperative epidemics. It can be seen that $\lambda_c^{II} \approx 0.039$ for $q = 0$, $\lambda_c^{II} \approx 0.042$ for $q = 0.2$, $\lambda_c^{II} \approx 0.044$ for $q = 0.5$ in Fig. 8(b)(ii) and $\lambda_c^{II} \approx 0.039$ for $q = 0$, $\lambda_c^{II} \approx 0.051$ for $q = 0.2$, $\lambda_c^{II} \approx 0.09$ for $q = 0.5$ in Fig. 8(c)(ii); obtained by simulation of epidemic dynamics. Compared with the immunization strategy, Fig. 8(c)(i) and (ii) shows that the effects of quarantine strategy in increasing the epidemic threshold and reducing the outbreak size is more significant, indicating that the quarantine strategy is more effective than the immunization strategy in suppressing epidemic spreading.

V. CONCLUSION

In this article, we focus on the cooperative epidemics, where the spread of one disease can enhance the spread of another disease. We introduced two self-awareness control strategies, immunization strategy and quarantine strategy, and studied their controlling effectiveness on the coinfection processes with the synergistic effect. We used the bond percolation theory to describe the SIR cooperative spreading model under the control strategies and investigated the

effects of the synergy factor and the control rate on the epidemic threshold and the outbreak size. Through the bond percolation theory and numerical simulations, we found that by increasing the synergy factor α, the effect of synergy enhances the spread of another disease when the two diseases meet, which enhances the epidemic threshold and reduces the outbreak size. On the ER random networks, the type of phase transition transforms from being continuous to discontinuous with the increase of synergy factor α. We got the critical synergy factor by the bifurcation analysis. When $\alpha \leq \alpha_c$, P_{ab} increases continuously with λ, and when $\alpha > \alpha_c$, the phase transition is discontinuous.

In terms of controlling diseases, both strategies can suppress the cooperative epidemics. For the immunization strategy, if there is no synergy mechanism, it has no effect on the epidemic threshold. If there is a synergy effect, the epidemic threshold will be increased and the type of phase transition is transformed from being discontinuous to continuous on ER random networks. For the quarantine strategy, no matter whether there is a synergy effect, the epidemic threshold can be increased. The quarantine strategy also transforms the type of phase transition from being discontinuous to continuous. Compared with the immunization strategy, the effects of quarantine strategy on cooperative epidemics are more significant, indicating that the quarantine strategy is more effective than the immunization strategy in suppressing epidemic dynamics. When fixing the synergy factor $\alpha = 3$, we get the critical control rate. For the immunization strategy, the critical rate is $q_s \approx 0.5$ on the simulated ER networks. When $0 \leq q \leq 0.5$, P_{ab} changes with λ discontinuously and P_{ab} changes with λ continuously when $0.5 < q \leq 1$. For the quarantine strategy, the critical rate is $q_s = 0.487$, which is a little less than that of immunization strategy.

We use bond percolation to provide the theoretical framework for the cooperative epidemics dynamics. The theoretical results and simulation results can be well matched, provided a correct theoretical basis for the cooperative epidemics. For controlling the spread of disease, we propose two self-awareness strategies, which has a very important practical significance. The cooperative spread of disease can be mapped to news and rumors, thus the results of this paper provides a theoretical guarantee for how to control the pervasion of rumors.

This paper mainly describes the cooperative epidemics on a single-layer network. However, multilayer networks have been one of the hotspots of complex network research in recent years.[40–47] Cooperative epidemics can be extended to multilayer networks to study the effects of the synergy factor, control strategies, and interlayer correlations on cooperative epidemics and phase. Moreover, the human activities and messages may influence disease transmission,[7,23,48,49] which can be mapped into cooperative epidemics.

ACKNOWLEDGMENTS

This work was supported by the National Natural Science Foundation of China (NNSFC) (Grant Nos. 11575041, 61673086, 61802321, 11075057, and 11875133), the Natural Science Foundation of Shanghai (Grant No. 18ZR1412200), and the Postdoctoral Research Fund of University of Electronic Science and Technology of China.

REFERENCES

[1] M. J. Keeling and P. Rohani, *Modeling Infectious Diseases in Humans and Animals* (Princeton University Press, 2008).
[2] W. Wang, M. Tang, H. E. Stanley, and L. A. Braunstein, Rep. Prog. Phys. **80**, 036603 (2017).
[3] M. E. J. Newman, Phys. Rev. Lett. **95**, 108701 (2005).
[4] S. Funk and V. A. A. Jansen, Phys. Rev. E **81**, 036118 (2010).
[5] Y.-B. Wang, G.-X. Xiao, and J. Liu, New J. Phys. **14**, 013015 (2011).
[6] C. Granell, S. Gómez, and A. Arenas, Phys. Rev. Lett. **111**, 128701 (2013).
[7] W. Wang, M. Tang, H. Yang, Y. Do, Y.-C. Lai, and G.-W. Lee, Sci. Rep. **4**, 5097 (2014).
[8] X.-T. Wei, N. C. Valler, B. A. Prakash, I. Neamtiu, M. Faloutsos, and C. Faloutsos, IEEE J. Sel. Areas Commun. **31**, 1049 (2013).
[9] M. E. Newman and C. R. Ferrario, PLoS One **8**, e71321 (2013).
[10] L. Chen, F. Ghanbarnejad, W. Cai, and P. Grassberger, Europhys. Lett. **104**, 50001 (2013).
[11] J. K. Taubenberger and D. M. Morens, Emerg. Infect. Dis. **12**, 15 (2006).
[12] C. K. Kwan and J. D. Ernst, Clin. Microbiol. Rev. **24**, 351 (2011).
[13] A. Pawlowski, M. Jansson, M. Sköld, M. E. Rottenberg, and G. Källenius, PLoS Pathog. **8**, e1002464 (2012).
[14] M. Belay, G. Bjune, and F. Abebe, Global Health Action **8**, 27949 (2015).
[15] M. Marvá, E. Venturino, and R. B. D. L. Parra, J. Appl. Math. **2015**, 275485 (2015).
[16] W. Cai, L. Chen, F. Ghanbarnejad, and P. Grassberger, Nat. Phys. **11**, 936 (2015).
[17] P. Grassberger, L. Chen, F. Ghanbarnejad, and W. Cai, Phys. Rev. E **93**, 042316 (2016).
[18] L. Hébertdufresne and B. M. Althouse, Proc. Natl. Acad. Sci. U.S.A. **112**, 10551 (2015).
[19] L. Chen, F. Ghanbarnejad, and D. Brockmann, New J. Phys. **19**, 103041 (2017).
[20] N. Azimi-Tafreshi, Phys. Rev. E **93**, 042303 (2016).
[21] H. K. Janssen and O. Stenull, Europhys. Lett. **113**, 26005 (2016).
[22] L. Chen, F. Ghanbarnejad, and D. Brockmann, New J. Phys. **19**, 103041 (2017).
[23] Q.-H. Liu, W. Wang, S.-M. Cai, M. Tang, and Y.-C. Lai, Phys. Rev. E **97**, 022311 (2018).
[24] P. Desjeux, Clin. Dermatol. **17**, 317 (1999).
[25] F. B. Agusto and I. M. Elmojtaba, PLoS One **12**, e0171102 (2017).
[26] H.-F. Zhang, J.-R. Xie, M. Tang, and Y.-C. Lai, Chaos **24**, 6872 (2014).
[27] J.-Q. Kan and H.-F. Zhang, Commun. Nonlinear Sci. **44**, 193 (2015).
[28] H.-F. Zhang, P.-P. Shu, Z. Wang, M. Tang, and M. Small, Appl. Math. Comput. **294**, 332 (2017).
[29] L. Lv, D.-B. Chen, X.-L. Ren, Q.-M. Zhang, Y.-C. Zhang, and T. Zhou, Phys. Rep. **650**, 1 (2016).
[30] R. Cohen, S. Havlin, and D. Benavraham, Phys. Rev. Lett. **91**, 247901 (2003).
[31] L. K. Gallos, F. Liljeros, P. Argyrakis, A. Bunde, and S. Havlin, Phys. Rev. E **75**, 045104 (2007).
[32] M. Catanzaro, M. Boguñá, and R. Pastorsatorras, Phys. Rev. E **71**, 027103 (2005).
[33] E. N. Gilbert, Anna. Math. Stat. **30**, 1141 (1959).
[34] M. E. J. Newman, Phys. Rev. E **66**, 016128 (2002).
[35] S. Boccaletti, G. Bianconi, R. Criado, C. del Genio, J. Gomez-Gardenes, M. Romance, I. Sendina-Nadal, Z. Wang, and M. Zanin, Phys. Rep. **544**, 1 (2014).
[36] W. Wang, M. Tang, H.-F. Zhang, and Y.-C. Lai, Phys. Rev. E **92**, 012820 (2015).
[37] M. E. J. Newman, *Networks: An Introduction* (Oxford University Press, 2010).
[38] P. Crépey, F. P. Alvarez, and M. Barthélemy, Phys. Rev. E **73**, 046131 (2006).
[39] P.-P. Shu, M. Tang, K. Gong, and Y. Liu, Chaos **22**, 043124 (2012).
[40] S. Boccaletti, G. Bianconi, R. Criado, C. I. D. Genio, J. Gómez-Gardeñes, M. Romance, I. Sendiña Nadal, Z. Wang, and M. Zanin, Phys. Rep. **544**, 1 (2014).
[41] M. Kivelä, A. Arenas, M. Barthelemy, J. P. Gleeson, Y. Moreno, and M. A. Porter, J. Complex Netw. **2**, 203 (2014).

[42]M. D. Domenico, C. Granell, M. A. Porter, and A. Arenas, Nat. Phys. **12**, 901 (2016).
[43]Z.-X. Wang, D. Zhou, and Y.-Q. Hu, Phys. Rev. E **97**, 032306 (2018).
[44]X.-L. Chen, R.-J. Wang, M. Tang, S.-M. Cai, H. E. Stanley, and L. A. Braunstein, New J. Phys. **20**, 013007 (2018).
[45]D.-W. Zhao, L.-H. Wang, Z. Wang, and G.-X. Xiao, IEEE Trans. Inf. Forensic Security **14**(7), 1755–1767 (2019).
[46]P.-C. Zhu, X.-G. Song, L.-B. Liu, Z. Wang, and J. Han, IEEE Access. **6**, 35292 (2018).
[47]P.-C. Zhu, Q. Zhi, Y.-M. Guo, and Z. Wang, "Analysis of epidemic spreading process in adaptive networks," IEEE Trans. Circuits Syst. II (published online).
[48]W. Wang, Q.-H. Liu, S.-M. Cai, M. Tang, L. A. Braunstein, and H. E. Stanley, Sci. Rep. **6**, 29259 (2016).
[49]Q.-H. Liu, W. Wang, M. Tang, and H.-F. Zhang, Sci. Rep. **6**, 25617 (2016).